



Universiteit
Leiden
The Netherlands

Cavity quantum electrodynamics with quantum dots in microcavities

Gudat, J.

Citation

Gudat, J. (2012, June 19). *Cavity quantum electrodynamics with quantum dots in microcavities*. *Casimir PhD Series*. Retrieved from <https://hdl.handle.net/1887/19553>

Version: Not Applicable (or Unknown)

License: [Licence agreement concerning inclusion of doctoral thesis in the Institutional Repository of the University of Leiden](#)

Downloaded from: <https://hdl.handle.net/1887/19553>

Note: To cite this publication please use the final published version (if applicable).

Cover Page



Universiteit Leiden



The handle <http://hdl.handle.net/1887/19553> holds various files of this Leiden University dissertation.

Author: Gudat, Jan

Title: Cavity quantum electrodynamics with quantum dots in microcavities

Issue Date: 2012-06-19

Appendices

Appendix A

Experimental setup

The original Helium-flow cryostat was designed for applications in ultra-high vacuum (UHV) (10^{-9} mbar) without any precision scanning technique implemented. For our needs we had to make modifications to fulfill our requirements of high thermal and physical stability over a long scanning time. Figure A.1 illustrates the basic cryostat without the micro-precision scanning stage mounted on top of the cryostat as described in Chap. 2 and illustrated in Fig. 2.2. The scheme shows the original top and bottom radiation heat shields reducing the heating impact of the thermal radiation from the environment, the original cooling braids (OFHC material) connecting the sample holder and the 4K pot for sufficient cooling of the sample and the rods (there are three of them) holding the 4K and the 60K pot in place. The rods thermally insulate the cold parts from the rest of the cryostat that is at room-temperature. Before we applied any modifications these three rods were the only physical connections holding the cold parts in place. The rods are made of Polyether Ether Ketone (PEEK) material which is well suited for UHV applications due to its very good thermal stability and low outgassing and vapor pressure.

Outgassing of materials is the main limiting factor with regard to the ultimate pressure which any particular system may reach assuming that leaks are absent. However, in our applications we do not necessarily have to measure at pressures below 10^{-6} mbar (high vacuum (HV) condition). The PEEK rods have the disadvantage that they are not as stiff as materials which are usually used for such designs operating at HV. In the same design the PEEK rods could be replaced with stainless steel rods. The Young's modulus of stainless steel is around (depending on the composition) ~ 200 GPa compared to $3.6 - 3.7$ GPa for PEEK making it much more suited for a stable setup (PEEK has a very low thermal conductivity at low temperatures of around $0.1 \frac{W}{m \cdot K}$ while stainless steel is $\sim 0.3 \frac{W}{m \cdot K}$ at around 4K; stainless steel allows thin wall machining that

can decrease the heat transfer). In scheme A.1 the Helium delivery line is partially drawn in the figure. A crucial design feature of the delivery line is the 30cm long mount that feeds the delivery line from the dewar to the cryostat. To cope with the thermal contraction of the delivery line during cooldown it is mounted on spring loads (as is the exhaust line not indicated in the scheme) that pushes all cooled parts in the horizontal direction. The problem that we encountered are small pressure changes and vibrations of the dewar causing large displacements of the sample-mount relative to the cryostat housing of up to $30\mu\text{m}$ due to the long level-arm of the delivery line. These large vibrations on a short term scale would complicate long term positioning measurements. To overcome these issues we installed a more sophisticated bottom radiation shield (see indication in Fig. A.1) that keeps the whole cooled pot in place by fixing it on the side-walls in the lower part of the cryostat. Heavy spring-loads pushing small stainless steel ball bearings against the wall minimize thermal conduction by keeping the contact surface as small as possible. The design improvement has proven to be able to allow nanometer-scale resolved scanning over a long time and at the same time to not reduce the cooling power needed for the whole setup (if at all, the temperature of the setup might only have increased on the order of 0.1K when at thermal equilibrium at the coldest possible temperature during comparable cooldown tests).

Another critical issue of our setup caused by the customized design changes was the ultimate cryogenic temperature and the time needed to reach thermal equilibrium. Initial tests without any modifications took around 90min to reach a final temperature of 12K measured at the top of the sample holder. The slow cooldown time was mainly caused by the limited cooling power through the Oxygen-free high thermal conductivity (OFHC) copper braids connecting the 4K pot with the sample holder. The micro-positioning xyz-stack is made of Titanium with a limited thermal conductivity of around $6\frac{\text{W}}{\text{m}\cdot\text{K}}$ compared to up to $10.000\frac{\text{W}}{\text{m}\cdot\text{K}}$ for OFHC copper at 4K. To increase the thermal conduction from the 4K pot to the sample holder we added additional (OFHC) copper braids with large contact areas between each micro-positioner as shown in picture A.2. The design reduced the cooldown time from 90min to 40min and still allows one to operate the positioners. Nevertheless, in order to reach a final temperature of close to 4.2K at the sample holder we had to make sure that all wires potentially causing a heat-sink would be cooled sufficiently before contacting the sample-holder or the sample. For that reason all wires are connected to the 60K pot before contact is made to the sample-holder as illustrated in Fig. A.3 where a few wires are tied down with dental floss (which has very good outgassing properties). Contacting the wires directly to the Helium transfer line (at 4K) resulted in less cooling power for the whole setup.

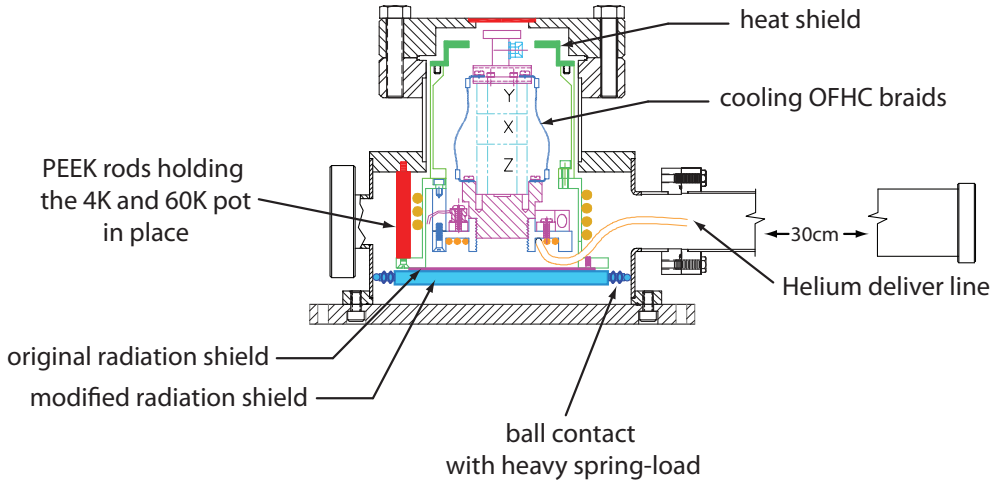


Figure A.1: Cryostat side view. Apart from the bottom radiation shield this is the original design of the customized cryostat. The sampler holder on top is located close to the optical window and can be positioned by the xyz-micropositioning stack. The Helium transfer line cooling the 4K and the 60K pot is illustrated by solid circles which coil horizontally (4K pot) and vertically (60K pot) in the center. Three PEEK rods (only one visible in the drawing) keep all cooled parts in place and connect to the room-temperature outerwall of the cryostat. The modified bottom radiation shield contacting the outer sidewalls of the cryostat with small spring-loaded balls were added as an improvement later. The helium delivery line enters the cryostat through a 30cm long tube from the right side.

A final improvement was to limit the impact of blackbody radiation from the objective (at room temperature) which is mounted very close to the sample. We utilized different customized radiation heat shields for the top of the 60K pot that allowed cooling of the sample to a minimum of 4.8K. Initially, we had the idea to cover the sample with a 100nm specially coated (reducing the impact by roughly 80% as we only investigate the sample at a wavelength range of 700 – 1000nm) thin diamond film. The impact of the shield design is very important. Figure A.4 displays the original heat shield on the left allowing cooling down to $\approx 12\text{K}$, the one in the middle allowed a final temperature of around 7 – 8K whereas the right design managed 4.8K.

The major literature source for improving the setup and understanding the system was the book *Matter and Methods at Low Temperature* [191] which serves as a very good reference for questions related to the issues addressed above.

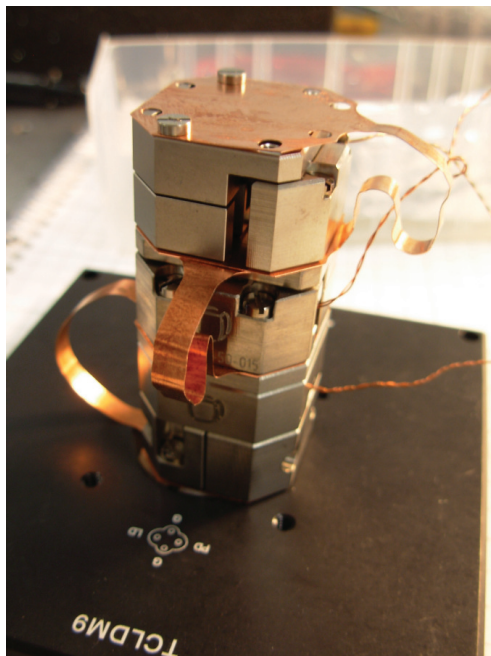


Figure A.2: xyz-micropositioning stack with additional copper braids for increased thermal conduction between each positioner and providing additional cooling power from the 4K pot to the sample holder.

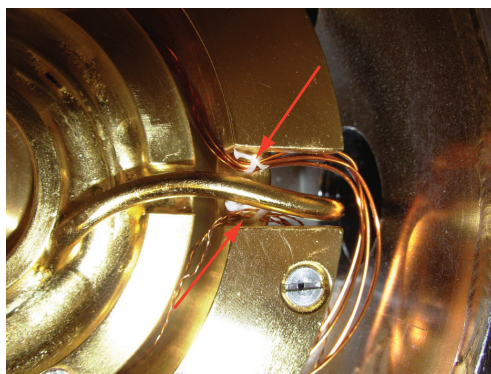


Figure A.3: Bottom view of the cryostat with the bottom radiation shield removed. Thermally contacting wires with the 60K pot by utilizing dental floss as tie downs as indicated by the arrows. The tube in the middle winding from right to left is the Helium transfer line which is the coldest part of the cryostat and cools the 4K pot in the center.



Figure A.4: Different radiation heat shield designs improving the final cooldown temperature of the sample from 12K (left) to 7 – 8K (center) to 4.8K (right).

